JVI Journals.ASM.org

Transfection of *Sclerotinia sclerotiorum* with *In Vitro* Transcripts of a Naturally Occurring Interspecific Recombinant of *Sclerotinia sclerotiorum* Hypovirus 2 Significantly Reduces Virulence of the Fungus

Shin-Yi Lee Marzano,[a] Houston A. Hobbs,[a] Berlin D. Nelson,[b] Glen L. Hartman,[a,c] Darin M. Eastburn,[a] Nancy K. McCoppin,[c] Leslie L. Domier[a,c]

Department of Crop Sciences, University of Illinois, Urbana, Illinois, USA[a]; Department of Plant Pathology, North Dakota State University, Fargo, North Dakota, USA[b]; United States Department of Agriculture/Agricultural Research Service, Urbana, Illinois, USA[c]

ABSTRACT

A recombinant strain of *Sclerotinia sclerotiorum* hypovirus 2 (SsHV2) was identified from a North American *Sclerotinia sclerotiorum* isolate (328) from lettuce (*Lactuca sativa* L.) by high-throughput sequencing of total RNA. The 5′- and 3′-terminal regions of the genome were determined by rapid amplification of cDNA ends. The assembled nucleotide sequence was up to 92% identical to two recently reported SsHV2 strains but contained a deletion near its 5′ terminus of more than 1.2 kb relative to the other SsHV2 strains and an insertion of 524 nucleotides (nt) that was distantly related to *Valsa ceratosperma* hypovirus 1. This suggests that the new isolate is a heterologous recombinant of SsHV2 with a yet-uncharacterized hypovirus. We named the new strain *Sclerotinia sclerotiorum* hypovirus 2 Lactuca (SsHV2L) and deposited the sequence in GenBank with accession number KF898354. *Sclerotinia sclerotiorum* isolate 328 was coinfected with a strain of *Sclerotinia sclerotiorum* endornavirus 1 and was debilitated compared to cultures of the same isolate that had been cured of virus infection by cycloheximide treatment and hyphal tipping. To determine whether SsHV2L alone could induce hypovirulence in *S. sclerotiorum*, a full-length cDNA of the 14,538-nt viral genome was cloned. Transcripts corresponding to the viral RNA were synthesized *in vitro* and transfected into a virus-free isolate of *S. sclerotiorum*, DK3. Isolate DK3 transfected with SsHV2L was hypovirulent on soybean and lettuce and exhibited delayed maturation of sclerotia relative to virus-free DK3, completing Koch's postulates for the association of hypovirulence with SsHV2L.

IMPORTANCE

A cosmopolitan fungus, *Sclerotinia sclerotiorum* infects more than 400 plant species and causes a plant disease known as white mold that produces significant yield losses in major crops annually. Mycoviruses have been used successfully to reduce losses caused by fungal plant pathogens, but definitive relationships between hypovirus infections and hypovirulence in *S. sclerotiorum* were lacking. By establishing a cause-and-effect relationship between *Sclerotinia sclerotiorum* hypovirus Lactuca (SsHV2L) infection and the reduction in host virulence, we showed direct evidence that hypoviruses have the potential to reduce the severity of white mold disease. In addition to intraspecific recombination, this study showed that recent interspecific recombination is an important factor shaping viral genomes. The construction of an infectious clone of SsHV2L allows future exploration of the interactions between SsHV2L and *S. sclerotiorum*, a widespread fungal pathogen of plants.

Sclerotinia sclerotiorum (Lib.) de Bary is a cosmopolitan fungal plant pathogen that causes necrotic diseases (e.g., *Sclerotinia* stem rot) in more than 400 plant species, which result in yield losses in major crops each year (1–3). However, the diseases caused by *S. sclerotiorum* have not been adequately controlled by conventional technologies thus far (4, 5). A number of mycoviruses have been molecularly characterized and associated with attenuation of the virulence of *S. sclerotiorum*, including a DNA virus (6, 7), a negative-sense RNA virus (8), mitoviruses (9, 10), and double-stranded RNA (dsRNA) (11) and single-stranded positive-sense RNA [ss(+)RNA)] viruses (12–17). Given the observations that mycoviruses transmitted intercellularly through hyphal anastomosis and extracellularly via viral particles can induce hypovirulence in *S. sclerotiorum* (7, 18), mycoviruses offer a promising approach to reduce crop damage caused by the fungus.

To date, two hypoviruses have been identified that infect *S. sclerotiorum*, *Sclerotinia sclerotiorum* hypovirus 1 (SsHV1) (17) and *Sclerotinia sclerotiorum* hypovirus 2 (SsHV2) (15, 16). SsHV1 was identified from *S. sclerotiorum* colonizing rapeseed (*Brassica napus* L.) and has a 10-kb RNA genome that contains a single large open reading frame (ORF) that encodes a polyprotein closely related to *Cryphonectria* hypovirus 3 (CHV3) and CHV4 (17). Cul-

Received 7 November 2014 **Accepted** 16 February 2015

Accepted manuscript posted online 18 February 2015

Citation Marzano S-YL, Hobbs HA, Nelson BD, Hartman GL, Eastburn DM, McCoppin NK, Domier LL. 2015. Transfection of *Sclerotinia sclerotiorum* with *in vitro* transcripts of a naturally occurring interspecific recombinant of *Sclerotinia sclerotiorum* hypovirus 2 significantly reduces virulence of the fungus. J Virol 89:5060–5071. doi:10.1128/JVI.03199-14.

Editor: A. Simon

Address correspondence to Leslie L. Domier, leslie.domier@ars.usda.gov.

doi:10.1128/JVI.03199-14

tures of *S. sclerotiorum* infected with SsHV1 also contained a 3.6-kb satellite RNA, the 5′ untranslated region (UTR) of which shared high nucleotide sequence identity with the 5′ UTR of SsHV1 (17). Based on comparisons of the dsRNA profiles and virulence properties of protoplast regenerants, SsHV1 alone did not appear to induce hypovirulence in *S. sclerotiorum*. Two strains of SsHV2, SsHV2/5472 and SsHV2/sx247, have been identified, one from *S. sclerotiorum* infecting tomato (*Solanum lycopersicum* L.) and one from *S. sclerotiorum* infecting rapeseed, respectively (15, 16). The genome sequences of the two SsHV2 strains contained single large ORFs that encoded polyproteins most closely related to the large polyprotein of CHV1. Both SsHV2-infected fungal isolates were originally coinfected with other mycoviruses (15, 16). The association of SsHV2 with hypovirulence also was characterized by comparing dsRNA patterns and relative virulence on host plants of fungal cultures derived from protoplast regenerants (15, 16). Unlike SsHV1, both SsHV2/5472 and SsHV2/sx247 were associated with reduced virulence in *S. sclerotiorum*, with greater variation in hypovirulence with SsHV2/5472.

Hypoviruses have been identified infecting four other fungal species, *Cryphonectria parasitica*, *Diaporthe* (syn. *Phomopsis*) *longicolla*, *Fusarium graminearum*, and *Valsa ceratosperma* (19–22). Despite what the family name implies, infection of fungal hosts by members of the *Hypoviridae* does not always induce hypovirulence. Three of the four hypoviruses of *C. parasitica*, CHV1, CHV2, and CHV3, and the two strains of SsHV2 have been associated with hypovirulence of their fungal hosts (15, 16, 23). In contrast, analysis of dsRNA patterns and virulence properties of multiple *C. parasitica* isolates suggested that CHV4 has little effect on fungal virulence (24). Similar analyses of dsRNA patterns and virulence properties suggested that *Fusarium graminearum* hypovirus 1 (FgHV1), *Phomopsis longicolla* hypovirus 1 (PlHV1), and *Valsa ceratosperma* hypovirus 1 (VcHV1) produced hypovirulence only when the fungal hosts were coinfected with separate satellite RNAs (20–22).

Because hypoviruses do not form particles for extracellular transmission, transfection of virus-free isolates with infectious full-genome cDNA clones is required to prove cause-and-effect relationships between hypovirus infection and hypovirulence. Only in the case of CHV1 has a virus-free fungal host been transfected with synthetic viral RNAs to demonstrate a cause-and-effect relationship between hypovirus infection and hypovirulence (25–27).

In this study, we identified a strain of SsHV2, named SsHV2L, from a North American isolate of *S. sclerotiorum* through a novel metatranscriptomic approach, chemically analyzed the secondary structure of its 5′ untranslated region (UTR), and characterized the relationship between SsHV2L and *S. sclerotiorum*. Two approaches were used to investigate whether SsHV2L induces hypovirulence in *S. sclerotiorum*. First, SsHV2L-infected *S. sclerotiorum* was treated with cycloheximide and hyphal tipped to produce a virus-free culture of the fungus. Second, protoplasts of a virus-free *S. sclerotiorum* isolate were transfected with full-length infectious transcripts of SsHV2L synthesized *in vitro*.

MATERIALS AND METHODS

Fungal isolates and growth conditions. A collection of 138 isolates of *S. sclerotiorum* from various hosts and locations in North America, maintained by the authors, was used in this research. Virus-infected isolate 328 was collected from lettuce in Arizona, USA, and virus-free *S. sclerotiorum* isolate DK3 was collected from soybean (*Glycine max* L. Merr.) in Illinois, USA (28). Cultures were maintained on potato dextrose agar (PDA) (Difco, Detroit, MI) at 22 to 24°C. For extraction of total RNA, cultures were grown in potato dextrose broth (PDB) for 5 to 7 days, and mycelia were collected on Whatman filter discs using Buchner funnels. One hundred milligrams of mycelia was transferred to 2-ml screw-cap tubes and frozen at −80°C until homogenization. Mycelia were homogenized with zinc-coated metal beads (3 mm in diameter) by dipping the tubes in liquid nitrogen for 10 s and pulverizing the tissue using a Mini Spec bead beater. The freezing in liquid nitrogen and beating were repeated until the mycelia were fully pulverized.

Extraction of total RNA and high-throughput sequencing (HTS). Total RNA was extracted from pulverized mycelia of 138 individually cultured field isolates of *S. sclerotiorum* using the RNeasy plant minikit (Qiagen, Valencia, CA). RNA samples were combined into three pools to facilitate identification of mycovirus-infected isolates and reduce the number of individual isolates that needed to be screened for individual mycoviruses. After depletion of the samples of rRNA with a Ribozero plant kit (Epicentre, Madison, WI), sequencing libraries were prepared from each of the three pooled RNA samples using the TruSeq stranded RNA sample preparation kit (Illumina, San Diego, CA). Libraries were quantitated by quantitative PCR (qPCR) and sequenced on three lanes for 101 cycles from each end of the fragments on an Illumina HiSeq 2000 sequencer using a TruSeq SBS sequencing kit version 3 (Illumina). FastQ files were generated with Casava 1.8.2 (Illumina), and reads with lengths of 100 nucleotides (nt) were used for *de novo* transcriptome assembly with Trinity (29). A multiple-kmer strategy was used for *de novo* transcriptome assembly, which increased contiguity and thus viral genome identification. kmers of 20, 25, and 30 were used. *Sclerotinia sclerotiorum*-derived sequences were removed by comparing the contigs to *S. sclerotiorum* gene models available from the *Sclerotinia sclerotiorum* Sequencing Project, Broad Institute of Harvard and MIT (http://www.broadinstitute.org/), using BLASTN (30). The remaining scaffolds were subjected to homology searches with BLASTX against the NCBI nonredundant amino acid sequence database.

RT-qPCR and RACE. When sequence reads from SsHV2L or SsEV1 were detected in an RNA pool, total RNA from each *S. sclerotiorum* isolate in that pool was analyzed by reverse transcriptase qPCR (RT-qPCR) with primers specific for SsHV2L (14576F [5′-GCGTTTGGCGTTCTCACTA T-3′] and 14675R [5′-CGACACTCTCATCGCTCAAG-3′]) or SsEV1 (80F [5′-TTTGGGTCCCTCTCAAAAGA-3′] and 200R [5′-TGGGGTTA GGCGTAAGTTTG-3′]) using the Power SYBR green RNA-to-CT 1-Step kit (Life Technologies, Grand Island, NY) in an ABI 7500 sequence detection system (Applied Biosystems, Foster City, CA) to determine which isolate(s) was infected with the viruses. To complete the genome sequence of SsHV2L, the 5′- and 3′-terminal sequences were determined using the FirstChoice RLM-RACE (rapid amplification of cDNA ends) kit (Life Technologies). Primers 315R (5′-TCTTCTAGGGCACTACTCCACAG A-3′) and 264R (5′-GAAAATTCAGGACCATCACGCACA-3′) were used for 5′ RACE as outer and inner primers, respectively. Primers 14391F (5′-ACATGTCAAGTCAAGAAGGGAGCA-3′) and 14604F (5′-GGTTA CCTTCCATCCCCTCTCTTC-3′) were used for 3′ RACE as outer and inner primers, respectively.

Phylogenetic and sequence analyses. For phylogenetic analyses, amino acid sequences of the large polyproteins of CHV1 (NP_041091), CHV2 (NP_613266), CHV3 (NP_051710), CHV4 (YP_13851), FgHV1 (YP_00901106Pl), PlHV1 (YP_009051683), SsHV1 (YP_004782527), SsHV2/5472 (YP_008828161), SsHV2L (KF898354), SsHV2/sx247 (AIA61616), and VcHV1 (YP_005476604) were downloaded from GenBank. The plum pox virus (NP_040807) polyprotein amino acid sequence was used as an outgroup to root trees. Sequences were aligned using MUSCLE (31), and neighbor-joining trees were constructed using MEGA 6.0 (32). GeneDoc (33) was used to calculate percent nucleotide and amino acid sequence identities to other hypovirus-like viruses. Recombination events were predicted using RDP4.36 (34) and the Recombination Analysis Tool (35).

The nucleotide sequences of the three SsHV2 isolates were aligned using MAFFT (36), and conserved protein domains were identified with the HMMER web server (37).

"Curing" of *S. sclerotiorum* isolate 328 of virus infections and virulence assays. *Sclerotinia sclerotiorum* 328 was cured of infection by SsHV2L and SsEV1 by growth on PDA amended with 355 μM cycloheximide on the lab bench at room temperature (22 to 24°C) without supplemental lighting for 10 days and hyphal tipping (38). Reductions in virus titers were evaluated by RT-qPCR with total RNA extracted from cycloheximide-treated cultures and electrophoretic analysis of dsRNA extracts. Colony morphologies on PDA and virulence levels on detached leaves of lettuce (*Lactuca sativa* L. var. longifolia) were compared. Young lettuce leaves (~5 cm long) were inoculated with each *S. sclerotiorum* isolate by placing a single 5-mm PDA disc from the edge of 4-day-old actively growing cultures on the center of a freshly harvested leaf. Two perpendicular measurements of lesion diameter were taken daily and averaged. The pair of isolates was compared twice with six and 30 replications for each trial, respectively. The GLM procedure of SAS ver. 9.4 (SAS Institute, Cary, NC) was used to compare lesion diameters produced by virus-free and virus-infected *S. sclerotiorum* cultures infected with SsEV1 and SsHV2L by Fisher's least significant difference test.

Construction of an infectious full-length clone of SsHV2L. A full-length cDNA clone of the SsHV2L genome was made from two overlapping cDNA fragments by RT-PCR from total RNA extracted from *S. sclerotiorum* isolate 328 infected with SsHV2L that were then joined via a native SacII site at position 5975. Specifically, cDNA was synthesized using primer 6890R (5′-ATGAGCACTCTGGCCAGGTATTC-3′) and total RNA as the template. The 5′ half of the SsHV2 genome was amplified using a 5′-specific forward primer (5′-TTTTTGGGGATGGTACTCTCA GGTTTGATC-3′) and 6012R (5′-AAAAGTTGGTGTGATGAATCCCT TCTCGATCTAC-3′) using iProof DNA polymerase (Bio-Rad Laboratories, Hercules, CA), cloned into pCR-Blunt II-TOPO (Life Technologies), gel purified, and digested with SacI and SacII. Using primer 3P [5′-GAG AGAGCTC$(T)_{26}$GCTTTTACGCGTTCACACCAT-3′], which contained a SacI recognition site (underlined), 26 T residues, and a sequence complementary to the 21 nt of SsHV2L immediately upstream of the poly(A) tail, cDNA was synthesized from total RNA. The 3′ half of the SsHV2L genome was amplified using primers 5898F (5′ CGTATTGTCAACAGG TGTGGCCTTCCTTTTATCACTTTTGGTCTGG-3′) and 3P, gel purified, and digested with SacI and SacII. Ligation of the two pieces resulted in a full-length cDNA clone of SsHV2L.

Transfection of *S. sclerotiorum* protoplasts with synthetic transcripts, virulence assay, and sclerotium quantification. The full-length clone of SsHV2L was cleaved with SacI and transcribed *in vitro* by T7 RNA polymerase using the mMessage mMachine T7 transcription kit (Life Technologies). Protoplasts were prepared from virus-free *S. sclerotiorum* isolate DK3 as described by Kohn et al. (39) with an enzyme digestion time of 3 h. Approximately 1.3×10^6 cells/100 μl were transfected with *in vitro* transcripts as previously described (25). Transfected protoplasts were plated on PDA and transferred weekly to fresh plates. Infection of *S. sclerotiorum* with SsHV2L was detected by RT-qPCR using total RNA extracted from fungal hyphae as described above and confirmed by analysis of dsRNA patterns.

Levels of growth and sclerotium production on PDA and virulence on detached leaves of lettuce and soybean (line LD9148) were compared for virus-free isolates DK3 and DK3 transfected with SsHV2L. One 5-mm PDA disc from the edge of a 4-day-old actively growing culture was inoculated onto the center of a fresh PDA plate. Numbers of sclerotia produced by the cultures were recorded in two trials of three and four replications a week after inoculation. For virulence assays, a single 5-mm PDA disc from the edge of a 4-day-old actively growing culture was placed on the center of a freshly harvested lettuce leaf or a detached center leaflet (4 to 5 cm long) from the first trifoliate leaf of a soybean seedling. All leaves were incubated at room temperature on a lab bench in sterile petri dishes without supplemental lighting. Two perpendicular measurements of lesion diameter were averaged daily.

Extraction of dsRNA. A modified procedure was used to purify dsRNA based on the method of Depaulo and Powell (40). The extracts were further purified to remove most of the single-stranded RNA and chromosomal DNA by CF-11 cellulose chromatography (41). The eluates were treated with S1 nuclease (Promega, Madison, WI) and Turbo DNase (Life Technologies) and visualized on 0.8% agarose gels.

TEM. Discs (5 mm) of mycelia from isolate 328, virus-free DK3, and DK3 transfected with SsHV2L grown on PDA were fixed in Karnovsky's fixative in phosphate-buffered 2% glutaraldehyde and 2.5% paraformaldehyde. Standard microwave procedures were used for embedding (42). The tissue was subjected to ultrathin sectioning, stained, and visualized for transmission electron microscopy (TEM) with a Hitachi H600 transmission electron microscope at the Frederick Seitz Materials Research Laboratory, University of Illinois.

Structure of the SsHV2L 5′ UTR. The secondary structure of the SsHV2L 5′ UTR was evaluated by selective 2′-hydroxyl acylation analyzed by primer extension (SHAPE) (43, 44). First, a template for *in vitro* transcription of an RNA corresponding to the 5′-terminal 428 nt of the SsHV2L genome was amplified using primers 5′-GAACCGGACCGAAG CCCGATTTGGATCCGGCGAACCGGATCGACGCACTGGTCTATTT CCAAGGGGG-3′ and 5′-GAGAGAGTGGTAATACGACTCACTATAG GGCCTTCGGGCCAATTTTTGGGGATG-3′, which added a T7 RNA polymerase promoter and bounding structures to the RNA template (43). The amplicon was transcribed *in vitro* by T7 RNA polymerase using the RiboMax large-scale RNA production system (Promega). RNA transcripts (36 pmol) were folded and treated with 12 mM or 20 mM *N*′-methylisatoic anhydride (NMIA) (dissolved in dimethyl sulfoxide [DMSO]) or DMSO alone for 45 min at 22°C or 37°C. 6-Carboxyfluorescein (FAM)- and hexachlorofluorescein (HEX)-labeled primers (5′-GAA CCGGACCGAAGCCCG-3′) complementary to the 3′ adapter (43) and FAM- and HEX-labeled primers complementary to nt 262 to 285 of the SsHV2L 5′ UTR were used for reverse transcription. Transcripts treated with NMIA or DMSO alone were extended with FAM-labeled primers. Untreated transcripts were reverse transcribed in the presence of ddCTP to generate a sequence ladder to align extension products to the reference sequence. Data were normalized and reactivities were calculated by QuShape (45). Reactivity values greater than 0.85 were used to constrain RNA secondary structure predictions by Mfold 2.3 (46). Nucleotide positions with reactivities between 4.0 and 0.85 were used to select between structures with similar free energies.

Nucleotide sequence accession numbers. We deposited the SsHV2L sequence in GenBank under accession number KF898354. The assembled sequence of SsEV1 from isolate 328 was deposited under GenBank accession number KC460912.

RESULTS

Metatranscriptomic identification of mycoviruses infecting *S. sclerotiorum*. Each HTS library produced from 5.3×10^7 to 1.7×10^8 100-nt reads. Homology searches of the assembled sequences against the NCBI virus amino acid sequence database using BLASTX identified contigs of 14,512 nt in the kmer = 25 and kmer = 30 assemblies from a pool of 64 *S. sclerotiorum* isolates that aligned with sequences of strains of SsHV2 from China (SsHV2/sx247, GenBank accession number KJ561218) and New Zealand (SsHV2/5472, GenBank accession number YP_008828161) (15, 16). A total of 20,322 100-nt reads aligned to each of the contigs for an average 140-fold depth of coverage. No sequence reads generated from the other two total RNA pools aligned to the contigs. Using primers designed based on the HTS assembly, RT-qPCR identified only *S. sclerotiorum* isolate 328 as infected with the virus. A second contig of 10,585 nt (GenBank accession number KM923990) was identified in the kmer = 25 assembly and con-

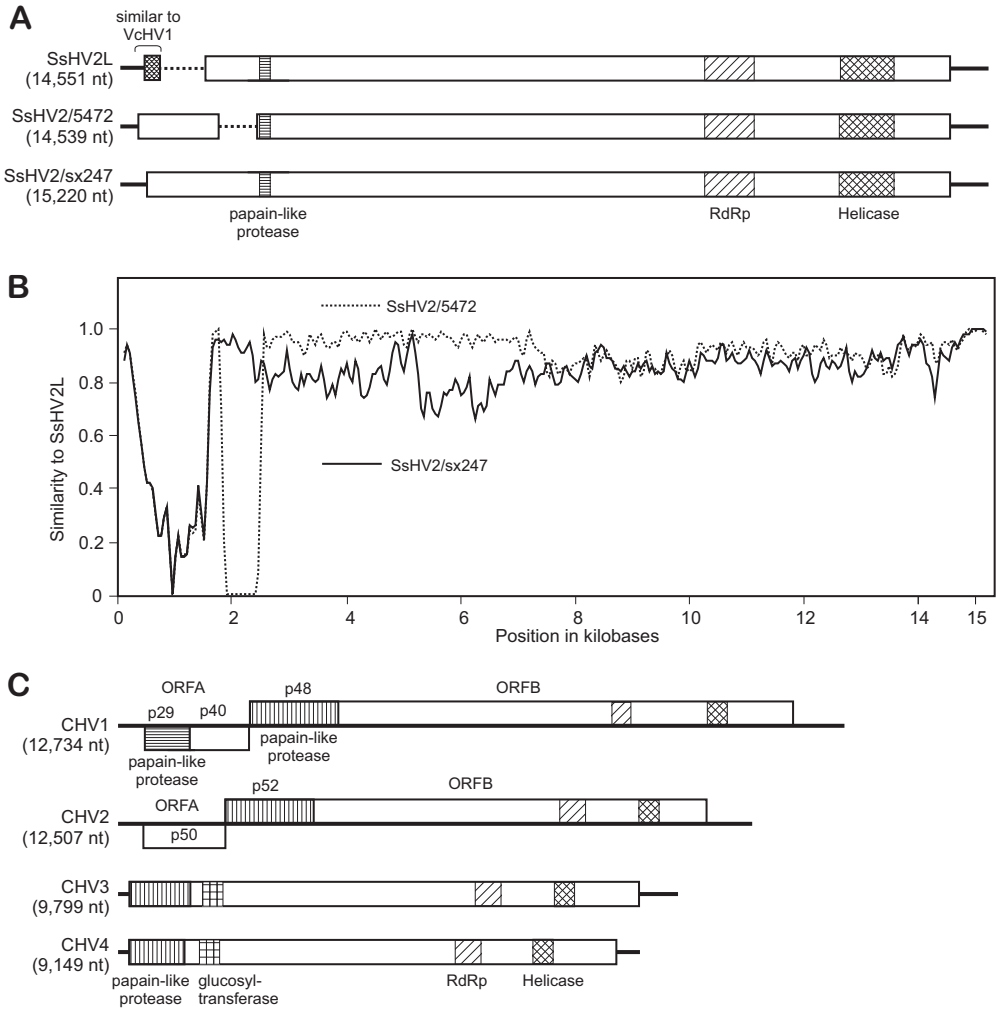

FIG 1 Comparisons of the organizations of three isolates of *Sclerotinia sclerotiorum* hypovirus 2 (SsHV2), isolates SsHV2L, SsHV2/5472, and SsHV2/sx247, with those of *Cryphonectria* hypoviruses 1, 2, 3, and 4 (CHV1, -2, -3, and -4). (A) Comparisons of the genome sequences of SsHV2L, SsHV2/5472, and SsHV2/sx247 showing the positions of deletions (dotted lines) and insertion of a sequence distantly related to *Valsa ceratosperma* hypovirus 1 (VcHV1) in SsHV2L. (B) Plot of the nucleotide sequence identities of SsHV2L with SsHV2/5472 and SsHV2/sx247 created with the Recombination Analysis Tool (35). (C) Genome organizations of CHV1, -2, -3, and -4. The positions of the glucosyl transferase, helicase, peptidase, and RNA-dependent RNA polymerase (RdRp) signature sequences are indicated for each open reading frame (ORF).

firmed to be present in isolate 328 by RT-qPCR with a nucleotide sequence that was 92% identical to SsEV1 (GenBank accession number KC852908) and 81% identical to *Sclerotinia sclerotiorum* endornavirus 2 (GenBank accession number KJ123645) (47). A total of 20,460 100-nt reads aligned to the contig for an average 193-fold depth of coverage. The assembled sequence represented 98% of the 10,770-nt SsEV1 genome. Hence, *S. sclerotiorum* isolate 328 was infected with two viruses, a hypovirus-like virus with a 14-kb genome and an endornavirus-like virus with a 10-kb genome. Rapid amplification of cDNA ends extended the hypovirus contig to 14,538 nt. We named the U.S. strain *Sclerotinia sclerotiorum* hypovirus 2 Lactuca (SsHV2L).

Molecular characterization and phylogenetic analysis of the hypovirus. The complete genome sequence of SsHV1L contained one 13,786-nt-long ORF that was predicted to encode a 519-kDa polyprotein. The ORF starts at the AUG triplet at nt 425 and ends with a UAG termination codon at nt 14209. As reported for SsHV2/5472 and SsHV2/sx247, the polyprotein was predicted to contain domains for a papain-like protease (nt 1798 to 2073), RNA-dependent RNA polymerase (RdRP; nt 9793 to 10437), and helicase (nt 11646 to 12894) (15, 16) (Fig. 1A). In addition, the first 86 residues of the SsHV2L polyprotein were 28% identical to the amino-terminal region of the VcHV1 polyprotein and contained a second domain conserved among C8 peptidases. The assembled sequence of SsEV1 from isolate 328 also contained a single long ORF starting at nt position 5 and extending to position 10480. The ORF was predicted to encode a polyprotein of 393 kDa that included domains for a methyltransferase (nt 809 to 1582), a DEAD-like helicase (nt 1012 to 3625), a viral RNA helicase (nt 5363 to 6052), and RdRp (nt 9191 to 9913).

Strain SsHV2L differed from SsHV2/sx47 and SsHV2/5472 by a 1.2-kb deletion near the 5′ terminus of the virus genome and insertion of 524 nt (Fig. 1A). The sequence of the 5′ UTR of SsHV2L diverged from those of the other two isolates beginning at position 313, which disrupted the first AUG codon for the large ORF in SsHV2L/sx247. The AUG codon at this position also was

TABLE 1 Percent nucleotide and amino acid sequence identity between SsHV2L and other confirmed and proposed members of the *Hypoviridae*

Virus	% sequence identity of virus[a]:										
	SsHV2L	SsHV2/sx247	SsHV2/5472	SsHV1	VcHV1	CHV1	CHV2	CHV3	CHV4	PlHV1	FgHV1
SsHV2L		84	85	11	11	10	10	10	10	10	9
SsHV2/sx247	80		85	11	11	10	10	11	10	10	9
SsHV2/5472	86	79		11	11	11	10	11	10	10	9
SsHV1	28	26	27		52	11	10	43	42	52	10
VcHV1	29	27	29	47		11	11	48	45	62	11
CHV1	27	26	27	24	25			10	10	10	19
CHV2	27	25	27	25	26	47		9	10	10	19
CHV3	29	28	29	48	53	25	26		36	49	10
CHV4	24	23	24	40	44	22	23	43		45	10
PlHV1	29	28	29	48	55	25	26	55	43		10
FgHV1	28	27	28	25	26	24	25	25	23	25	

[a] Values above the diagonal are nucleotide identity; values below the diagonal are amino acid identity.

not conserved in SsHV2/5472. At position 845, the SsHV2L nucleotide sequence resumed aligning to SsHV2/sx47 and SsHV2/5472 at positions 1527 and 1529, respectively. Therefore, the SsHV2L nucleotide sequence contained a deletion of 1,216 and 1,215 nt relative to SsHV2/sx47 and SsHV2/5472, respectively. In addition, SsHV2/5472 appeared to contain a 672-nt deletion relative to SsHV2L and SsHV2/sx47, which starts at position 1763 in the SsHV2/5472 sequence. SsHV2L shared 86% and 93% identity in nucleotide sequences in 96% and 91% of its genome to SsHV2/sx247 and SsHV2/5472, respectively. As mentioned above, the predicted amino acid sequence of the 524-nt insertion in SsHV2L was more similar to, but clearly distinct from, the amino acid sequence of the amino-terminal region of the polyprotein encoded by VcHV1 than to those of SsHV2/sx47 or SsHV2/5472 (Fig. 1B). The divergence of the SsHV2L nucleotide sequence from those of SsHV2/5472 and SsHV2/sx47 suggests that the 5′ recombination breakpoint with the hypovirus similar to VcHV1 is located between positions 312 and 313 in the 5′ UTR of SsHV2L.

Besides being up to 92% identical to SsHV2/5471 and SsHV2/sx247, the SsHV2L polyprotein sequence was 10% identical to CHV1 and CHV2 and 9% to FgHV1 (Table 1). A neighbor-joining tree based on alignment of full-length amino acid sequences of the eight reported hypovirus-like viruses showed relationships similar to those previously described for SsHV2 where SsHV2L was within a clade separate from CHV3, CHV4, SsHV1, and VcHV1 (15, 16) (Fig. 2). However, its genome structure (Fig. 1C) was more similar to CHV3 and CHV4, which have a single ORF, than to CHV1 and CHV2, which have two overlapping ORFs.

Effects of SsHV2L infection on fungal growth and virulence. The levels of growth in culture and virulence on plants were compared for the original *S. sclerotiorum* isolate 328 that was coinfected with SsEV1 and SsHV2L and isolate 328 cured of mycovirus infection. Analysis of SsHV2L RNA content of *S. sclerotiorum* cultures by RT-qPCR produced average threshold cycle (C_T) values for cycloheximide-treated cultures of greater than 35 compared to an average of less than 16 for cultures infected with SsHV2L. This represented at least a 5×10^5-fold reduction in SsHV2L RNA content in the cycloheximide-treated cultures. Compared to the original *S. sclerotiorum* isolate 328 that was infected with SsEV1 and SsHV2L, cultures of cured isolate 328 showed darker pigmentation in both mycelia and sclerotia and enhanced production of sclerotia (Fig. 3A). In detached leaf assays on lettuce, average lesion diameters caused by cycloheximide-treated isolate 328 were significantly larger than those caused by the original isolate 328 ($P < 0.05$) (Fig. 3B and C).

To establish a cause-and-effect relationship between SsHV2L infection and hypovirulence in *S. sclerotiorum*, protoplasts of a virus-free *S. sclerotiorum* isolate, DK3, were transfected with SsHV2L *in vitro* transcripts. Transfection of isolate DK3 with *in vitro* transcripts of SsHV2L was verified by RT-qPCR (average $C_T = 18$) and dsRNA analysis. As expected from the HTS data,

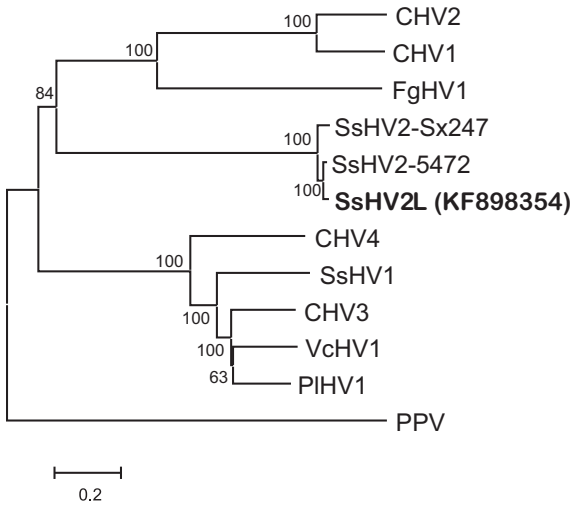

FIG 2 Neighbor-joining tree depicting the relationships of the predicted amino acid sequences of the large polyproteins of SsHV2L and other confirmed and proposed members of the *Hypoviridae*. Large polyprotein amino acid sequences of *Cryphonectria* hypovirus 1 (CHV1, NP_041091), *Cryphonectria* hypovirus 2 (CHV2, NP_613266), *Cryphonectria* hypovirus 3 (CHV3, NP_051710), *Cryphonectria* hypovirus 4 (CHV4, YP_13851), *Fusarium graminearum* hypovirus 1 (FgHV1, YP_00901106Pl), *Phomopsis longicolla* hypovirus1 (PlHV1, YP_009051683), *Sclerotinia sclerotiorum* hypovirus 1 (SsHV1, YP_004782527), *Sclerotinia sclerotiorum* hypovirus 2/5472 (SsHV2/5472, AHA56680), *Sclerotinia sclerotiorum* hypovirus 2L (SsHV2L, KF898354), *Sclerotinia sclerotiorum* hypovirus 2/sx247 (SsHV2-sx247, YP_008828161), and *Valsa ceratosperma* hypovirus 1 (VcHV1, YP_005476604) were aligned with MUSCLE, and trees were inferred using MEGA6. Horizontal branch lengths are scaled to the expected underlying number of amino acid substitutions per site. Bootstrap percentages of clades are shown (when approximately >50%) along internal branches of the trees. Topologies of the bootstrap majority-rule consensus trees were identical to those inferred from the nonresampled data sets. The plum pox virus (PPV) polyprotein amino acid sequence was used as an outgroup to root the tree.

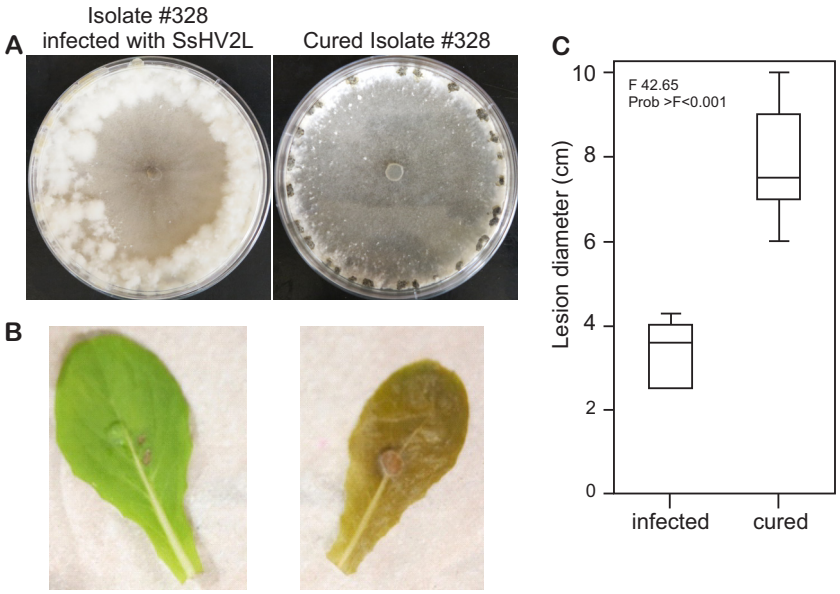

FIG 3 Comparison of the growth and virulence of *Sclerotinia sclerotiorum* isolate 328 infected with SsHV2L and SsEV1 and isolate 328 cured of mycovirus infection. (A) Colony morphology of *S. sclerotiorum* grown on potato dextrose agar at 22°C for 10 days. (B) Comparison of *S. sclerotiorum* virulence on detached lettuce leaves inoculated with agar plugs containing the pathogen and incubated at 22°C for 72 h. (C) Box plot comparison of mean lesion diameters (cm) on detached lettuce leaves from one of the two trials measured at 48 h after inoculation with mycelial agar plugs.

dsRNA extracted from *S. sclerotiorum* isolate 328 contained two bands, a 14-kb band corresponding to SsHV2L and a 10-kb band corresponding to SsEV1 (Fig. 4A). Double-stranded RNA extracted from transfected isolate DK3 contained a 14-kb dsRNA band corresponding to SsHV2L but not the 10-kb dsRNA band from SsEV1. The 10-kb dsRNA band was not observed in isolate DK3 transfected with SsHV2L *in vitro* transcripts even after multiple passages. These results indicated that SsHV2L replicative-form RNA was produced after transfection with the ss(+)RNA transcripts and that the RNA transcripts were infectious. In detached leaf assays, lesions produced by virus-free DK3 were significantly ($P < 0.0005$) larger than those produced by DK3 transfected with SsHV2L on both soybean and lettuce leaves (Fig. 4B and D). Significantly ($P < 0.05$) fewer sclerotia were produced, and their production was notably delayed, in isolate DK3 transfected with SsHV2L compared to virus-free DK3 (Fig. 4C). In a trial of four replications, virus-free DK3 produced 52 sclerotia, more than twice that, 22, of SsHV2L/DK3 cultures (Fig. 4D).

Electron microscopy of virus-infected and virus-free mycelia. Thin sections of mycelia from isolate DK3 transfected with SsHV2L contained lipid vesicles with diameters of 30 to 40 nm located proximal to cell walls (Fig. 5B) that were not observed in sections of virus-free DK3 (Fig. 5A). The sizes were similar to those observed in hypovirus-infected *C. parasitica* (48–50). Images of sections from *S. sclerotiorum* isolate 328 coinfected with SsEV1 and SsHV2L contained lipid vesicles with diameters of 50 to 60 nm within nuclei (Fig. 5C and D) that were not present in SsHV2L-transfected DK3.

Recombination and secondary structure. In agreement with sequence alignments described above, RDP4 analysis of amino acid sequences of the eight assigned and tentative members of the *Hypoviridae* predicted one significant ($P = 0.01$) interspecific recombination event near the 5′ end of the genome between the progenitor of SsHV2L (possibly SsHV2/5427) and an unknown major parent related to VcHV1 to form SsHV2L. Additionally, RDP4 analyses of the aligned nucleotide sequences of the three SsHV2 isolates detected significant intraspecific events that involved the unknown major parent related to SsHV2/5427 and SsHV2/sx247 as the minor parent ($P < 10^{-7}$) beginning at nt 4551 and ending at nt 7453 in SsHV2L. Within this region, the SsHV2L sequence was 96% identical to SsHV2/5427 but only 81% identical to SsHV2/sx247. In contrast, the region of the SsHV2L genome downstream of nt 7454 was on average 90% and 86% identical to SsHV2/5427 and SsHV2/sx247, respectively (Fig. 1B).

Predictions of the structure of the 5′ UTRs of SsHV2L constrained by reactivity with NMIA showed that the region contained multiple stem-and-loop structures that were stable at both 22°C and 37°C (Fig. 6). A subset of the structures were similar to the prediction reported by Khalifa and Pearson (16). The RNA secondary structure derived from the SHAPE data included a large stem-and-loop structure spanning positions 268 through 338 that included the putative breakpoint for recombination with the VcHV1-like virus (Fig. 1). In the RNA fragment analyzed, the AUG codon at position 425 was predicted to be unpaired.

DISCUSSION

High-throughput sequencing technologies for metagenomics have opened a new era for discovery of viruses that are relatively undersurveyed in nature (51–54), including mycoviruses (55). In this study, bioinformatic analysis of HTS data was used to assemble a nearly complete genome sequence of a recombined isolate of SsHV2 and SsEV1 without first purifying dsRNA. This allowed the unbiased detection of mycoviruses infecting the different *S. sclerotiorum* isolates. The North American strains of SsHV2 and SsEV1 discovered were two of more than 50 novel mycoviruses that were identified using HTS in these analyses (S. L. Marzano, B. D. Nelson, O. Ajayi, C. A. Bradley, T. J. Hughes, G. L. Hartman, D. M. Eastburn, and L. L. Domier, unpublished data). Similarly,

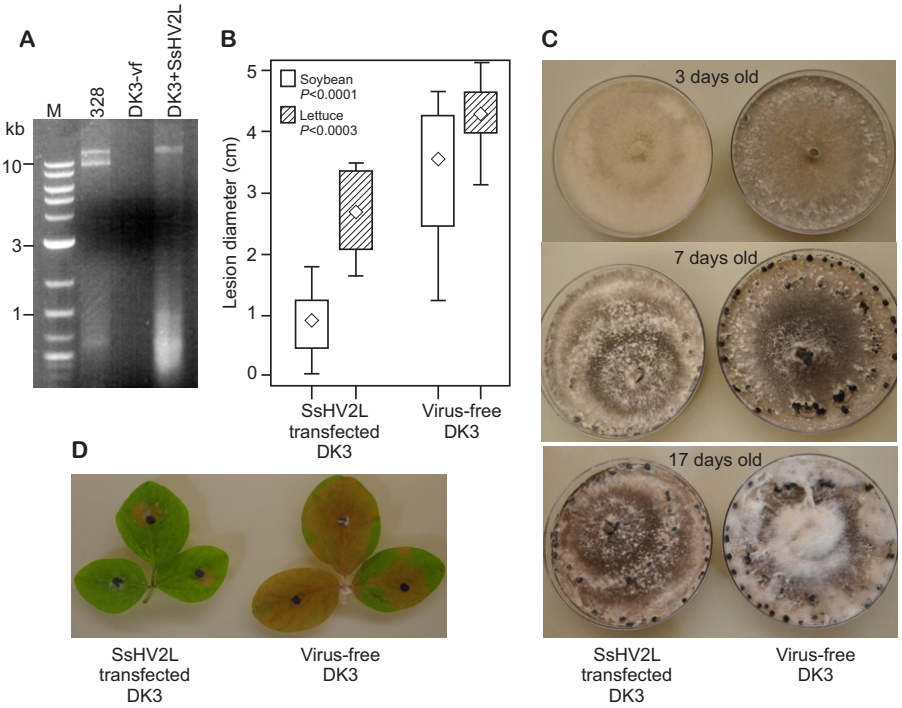

FIG 4 Comparison of the growth and virulence of virus-free *Sclerotinia sclerotiorum* isolate DK3 and isolate DK3 transfected with SsHV2L. (A) Agarose gel of dsRNAs from *S. sclerotiorum* isolates 328, virus-free DK3, and DK3 transfected with *in vitro* transcripts from a full-length cDNA clone of SsHV2L (0.8% gel; 3-h running time). All samples were purified by CF-11 cellulose chromatography and treated with DNase I. Sizes of DNA ladder standards (lane M) are indicated in kilobase pairs (kb). (B) Box plot comparisons of mean lesion diameters (cm) at 72 h after inoculation with mycelial agar plugs on detached soybean (30 biological replicates) and lettuce (eight biological replicates) leaves. (C) Comparison of colony morphologies of virus-free *S. sclerotiorum* isolate DK3 and isolate DK3 transfected with SsHV2L grown on potato dextrose agar for 3, 7, and 17 days at 22°C. (D) Attenuation of *S. sclerotiorum* virulence by SsHV2L on detached soybean leaves at 48 h after inoculation with mycelial agar plugs at 22°C.

HTS analysis of the transcriptomes of field-grown grape (*Vitis vinifera* L.) identified 26 putative mycoviruses infecting grape-associated fungi (56). The nearly complete genome sequence assembled from HTS made RACE reactions to determine the full-length genome straightforward and facilitated the construction of a full-length infectious cDNA clone of the viral genome, which allowed us to establish a cause-and-effect relationship for the attenuation of *S. sclerotiorum* virulence by SsHV2.

Similar to observations with other fungi infected with hypoviruses, polyadenylated genomic RNAs of SsHV2L do not encode structural proteins and are not packaged in proteinaceous virus particles (57). Instead, fungal cells infected with CHV1 contain pleomorphic lipid vesicles with diameters of 50 to 80 nm that contain viral dsRNA and replicase protein (58–60). Similar membrane structures were observed in the cytoplasm of *S. sclerotiorum* isolate DK3 transfected with SsHV2L and in nuclei of isolate 328 naturally coinfected with both SsHV2L and SsEV1. While it is possible that the nucleus-localized vesicles were produced by SsEV1, subcellular fractionation studies indicated that membrane vesicles associated with endornavirus infections were localized within the cytoplasm (61, 62).

Infection of fungi with multiple mycoviruses is common, which complicates the association of a particular mycovirus with a change in fungal virulence because of potential interactions of the mycoviruses and the possibility of additive or synergistic effects (23, 63). Cultures of *S. sclerotiorum* from which SsHV2/sx247 was isolated were coinfected with an alphaflexivirus (15), and cultures infected with SsHV2/5427 were coinfected with an endornavirus and a negative-sense RNA virus (16). Protoplast-regenerant cultures of *S. sclerotiorum* containing only dsRNAs from SsHV2/sx247 were hypovirulent on rapeseed, but it was not clear whether coinfection with the alphaflexivirus increased hypovirulence (15). Khalifa and Pearson (47) found that protoplast-derived cultures of *S. sclerotiorum* containing only dsRNAs from SsHV2/5427 were less hypovirulent on tomato than cultures that appeared to be coinfected with SsHV2/5427 and the endornavirus. In this study, both HTS and dsRNA data indicated that *S. sclerotiorum* isolate 328 was infected with strains of SsHV2 and SsEV1. To fully elucidate their roles in hypovirulence, an infectious clone of SsEV1 would have to be made to characterize the interaction between the two viruses.

Inter- and intraspecific recombination have played important roles in speciation and emergence of new variants in multiple virus lineages, including hypoviruses (19, 20, 64–67). Likewise, strains of SsHV2 appear to have multiple intra- and interspecific recombination and deletion events. The comparatively greater variation in the 5′ terminus of SsHV2 strains resembles the greater variation among *Cryphonectria* hypoviruses (Fig. 1C). Alignments of the nucleotide and amino acid sequences of SsHV2L to other hypoviruses suggested that it is the product of an interspecific recombination event that involved the papain-like protease between an SsHV2 isolate and a hypovirus distantly related to VcHV1. In a similar manner, the genome of FgHV1 appears to be recombinant, with its 5′-proximal ORF derived from a virus sim-

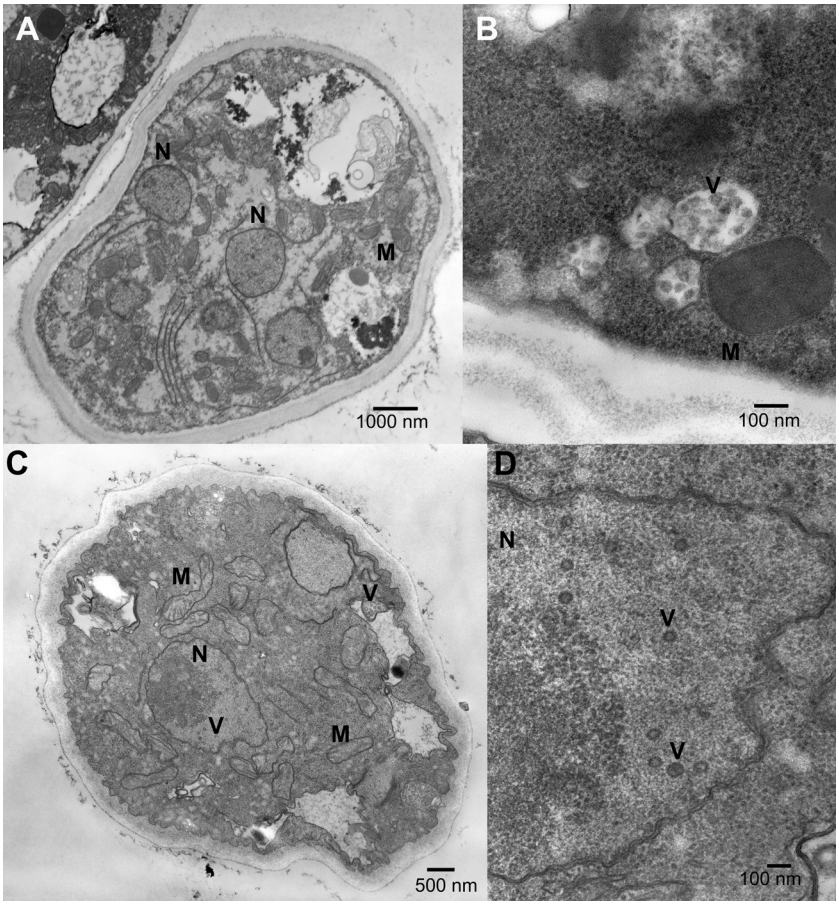

FIG 5 Transmission electron micrographs of thin sections of *Sclerotinia sclerotiorum* isolates 328 and DK3 showing the degradation of mitochondria (M) and of nuclei (N) and the formation of lipid vesicles (V) associated with mycovirus infection. Cross sections through mycelia of virus-free *S. sclerotiorum* isolate DK3 (A), isolate DK3 transfected with SsHV2L showing vesicles associated with cell walls (B), and isolate 328 infected with SsHV2L and SsEV1 (C) and a high-magnification image of isolate 328 infected with SsHV2L and SsEV1 showing vesicles associated with the nucleus and cytoplasm (D).

ilar to CHV4 and VcHV1 and its larger 3′-proximal ORF derived from a virus similar to CHV1 and CHV2 (20). For these recombination events to have occurred, a fungal host must have been infected with both viruses to allow the cross-species exchange. All three *S. sclerotiorum* isolates infected with SsHV2 were coinfected with other mycoviruses, suggesting that mixed mycovirus infections are common in *S. sclerotiorum* and thus provide opportunities for interspecific recombination.

Like CHV1, the 5′ noncoding region of SsHV2/5472 was predicted to contain multiple stem-and-loop structures that resemble internal ribosome entry sites (IRES) (16, 68). Probing the structure of the SsHV2L 5′ UTR by SHAPE indicated that the region contained multiple highly stable stem-and-loop structures, the largest of which contained the putative recombination event with the hypovirus related to VcHV1. Stem-and-loop structures have been shown to be important for similarity-nonessential recombination in RNA viruses (69–71). Because the 5′ UTRs of hypoviruses often are highly structured, it is possible that stem-and-loop structures in this region facilitated the shift of viral replicase from the RNA of one progenitor virus species to the other during virus replication. Both host and virus factors have been shown to be involved in RNA-RNA recombination of hypoviruses in *C. parasitica*, including a host Argonaute enzyme and viral RNA silencing suppressor (RSS) (72, 73). Additional studies are needed to evaluate the roles of secondary structures in the 5′ UTR of SsHV2 in translation initiation and recombination.

Strains of SsHV2 varied in the degree to which they attenuated growth culture and aggressiveness on plants of *S. sclerotiorum* (15, 16). Unlike SsHV2/sx247, SsHV2L infection did not cause a complete loss of sclerotium production. Instead, *S. sclerotiorum* infected with SsHV2L showed reduced and delayed production of sclerotia. Hence, SsHV2L may not be as debilitating as SsHV2/sx247. The difference in sclerotium production between these two strains of the viruses may be due to differences in the 5′-proximal regions. To evaluate the relative contributions of different portions of the SsHV2 genome to variations in the abilities of the two isolates to induce hypovirulence, chimeric viruses can be engineered (26, 74). Such analyses could also elucidate interactions between the hypovirus and its fungal host that could be used to enhance the biocontrol potential of the virus.

Like the p29 protein encoded by ORF A of CHV1, the amino-terminal regions of the polyproteins of the three isolates of SsHV2 contained sequences similar to the active sites of papain-like proteases. In CHV1, p29 is dispensable for viral replication, but deletion of the p29 coding sequence resulted in enhanced pigmentation and conidiation relative to wild-type CHV1, suggesting that

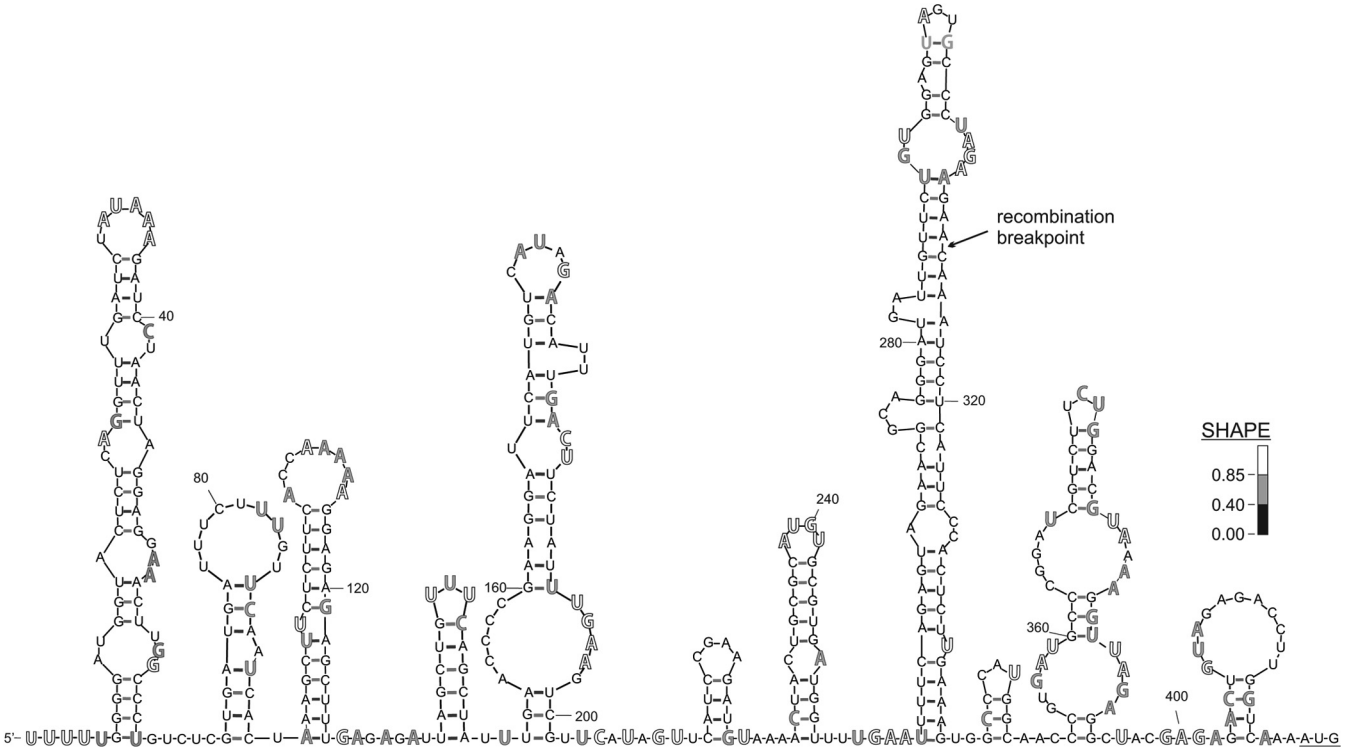

FIG 6 Secondary structure model for the 5′ untranslated region (nt 1 to 428) of the *Sclerotinia sclerotiorum* hypovirus 2L (SsHV2L) genome. Nucleotides are highlighted according to their SHAPE reactivity: black letters, low reactivity; gray letters, medium reactivity; white-filled letters, strong reactivity. The position of the putative 5′ recombination breakpoint in SsHV2L with a virus distantly related to *Valsa ceratosperma* hypovirus 1 is indicated in the large stem-loop structure beginning at nt 265.

p29 is a major symptom determinant for CHV1 (75). The p29 protease of CHV1 has been shown to function as an RSS and share functional and sequence similarities with the helper-component proteases of potyviruses, which also suppress host RNA silencing and are major virulence determinants (76, 77). Similar to experimentally generated deletions in the p29 coding sequence of CHV1 (78), SsHV2L and SsHV2/5472 contain deletions proximal to the putative active site of the protease yet still replicated in *S. sclerotiorum*. The presence of deletions in the region of the genomes of SsHV2L and SsHV2/5472 putatively encoding a major symptom determinant may partially explain why *S. sclerotiorum* infected with SsHV2L or SsHV2/5472 produced sclerotia but *S. sclerotiorum* infected with SsHV2/sx247 did not. The reduction in pigmentation in *S. sclerotiorum* isolates infected with SsHV2L may result from RNA silencing-mediated disruption of polyketide synthase gene expression that is required for melanin biosynthesis (79), which in turn could result in faster degradation of sclerotia in soil (80). Additional studies are needed to identify the RSS expressed by SsHV2 and investigate its potential role in suppression of pigmentation and sclerotium production. Identification of the RSS could lead to a further understanding of how RNA mycoviruses disrupt the antiviral defenses of their fungal hosts and effects on host gene expression that lead to alterations in fungal growth, morphology, and virulence (73, 81).

Vegetative incompatibility in fungi is thought to function to reduce transmission of harmful cytoplasmic genetic elements, including parasitic nuclei, transposable elements, and mycoviruses (82). Multiple studies have documented the existence of large numbers of *S. sclerotiorum* mycelial compatibility groups (MCGs) within relatively narrow geographic regions (28, 39, 83). The large numbers of MCGs could limit spread of mycoviruses in *S. sclerotiorum* or, as suggested by Brusini and Robin (84), provide a discontinuous network through which mycoviruses could spread in the field. Genes for vegetative incompatibility often are hypervariable and appear to be under diversifying selection (82). Taking advantage of this hypervariability and genetic markers associated with vegetative incompatibility phenotypes, six *vic* genes were identified in *C. parasitica* that limit the horizontal transmission of CHV1 (85, 86). The *S. sclerotiorum* genome contains a large repertoire of genes putatively involved in vegetative incompatibility (87), which is likely responsible for the high diversity of MCGs observed in the field and the difficulty of associating molecular markers with particular MCGs in *S. sclerotiorum* (39, 88–91). Disruption of the expression of genes for vegetative incompatibility through virus-induced gene silencing could facilitate the spread of SsHV2L or other hypovirulence-inducing mycoviruses through incompatible populations. The construction of a cDNA infectious clone of SsHV2 may facilitate such disruptions of gene expression in *S. sclerotiorum* and eventually provide biocontrol alternatives and knowledge toward understanding the pathways involved in hypovirulence caused by SsHV2.

ACKNOWLEDGMENTS

This research was funded by the National Sclerotinia Initiative and the United States Department of Agriculture/Agricultural Research Service.

Mention of a trademark, proprietary product, or vendor does not

constitute a guarantee or warranty of the product by the United States Department of Agriculture or the University of Illinois and does not imply its approval to the exclusion of other products or vendors that may also be suitable.

REFERENCES

1. **Boland GJ.** 2004. Fungal viruses, hypovirulence, and biological control of *Sclerotinia* species. Can J Plant Pathol **26:**6–18. http://dx.doi.org/10.1080/07060660409507107.
2. **Purdy LH.** 1979. *Sclerotinia sclerotiorum*: history, diseases and symptomatology, host range, geographic distribution, and impact. Phytopathology **69:**875–880. http://dx.doi.org/10.1094/Phyto-69-875.
3. **Steadman JR.** 1979. Control of plant-diseases caused by *Sclerotinia* species. Phytopathology **69:**904–907. http://dx.doi.org/10.1094/Phyto-69-904.
4. **Bardin SD, Huang HC.** 2001. Research on biology and control of *Sclerotinia* diseases in Canada. Can J Plant Pathol **23:**88–98. http://dx.doi.org/10.1080/07060660109506914.
5. **Boland GJ, Hall R.** 1994. Index of plant hosts of *Sclerotinia sclerotiorum*. Can J Plant Pathol **16:**93–108. http://dx.doi.org/10.1080/07060669409500766.
6. **Yu X, Li B, Fu YP, Jiang DH, Ghabrial SA, Li GQ, Peng YL, Xie JT, Cheng JS, Huang JB, Yi XH.** 2010. A geminivirus-related DNA mycovirus that confers hypovirulence to a plant pathogenic fungus. Proc Natl Acad Sci U S A **107:**8387–8392. http://dx.doi.org/10.1073/pnas.0913535107.
7. **Yu X, Li B, Fu Y, Xie J, Cheng J, Ghabrial SA, Li G, Yi X, Jiang D.** 2013. Extracellular transmission of a DNA mycovirus and its use as a natural fungicide. Proc Natl Acad Sci U S A **110:**1452–1457. http://dx.doi.org/10.1073/pnas.1213755110.
8. **Liu LJ, Xie JT, Cheng JS, Fu YP, Li GQ, Yi XH, Jiang DH.** 2014. Fungal negative-stranded RNA virus that is related to bornaviruses and nyaviruses. Proc Natl Acad Sci U S A **111:**12205–12210. http://dx.doi.org/10.1073/pnas.1401786111.
9. **Khalifa ME, Pearson MN.** 2013. Molecular characterization of three mitoviruses co-infecting a hypovirulent isolate of *Sclerotinia sclerotiorum* fungus. Virology **441:**22–30. http://dx.doi.org/10.1016/j.virol.2013.03.002.
10. **Xie JT, Ghabrial SA.** 2012. Molecular characterizations of two mitoviruses co-infecting a hypovirulent isolate of the plant pathogenic fungus *Sclerotinia sclerotiorum*. Virology **428:**77–85. http://dx.doi.org/10.1016/j.virol.2012.03.015.
11. **Xiao XQ, Cheng JS, Tang JH, Fu YP, Jiang DH, Baker TS, Ghabrial SA, Xie JT.** 2014. A novel partitivirus that confers hypovirulence on plant pathogenic fungi. J Virol **88:**10120–10133. http://dx.doi.org/10.1128/JVI.01036-14.
12. **Liu HQ, Fu YP, Jiang DH, Li GQ, Xie J, Peng YL, Yi XH, Ghabrial SA.** 2009. A novel mycovirus that is related to the human pathogen hepatitis E virus and rubi-like viruses. J Virol **83:**1981–1991. http://dx.doi.org/10.1128/JVI.01897-08.
13. **Xie J, Wei DM, Jiang DH, Fu YP, Li GQ, Ghabrial S, Peng YL.** 2006. Characterization of debilitation-associated mycovirus infecting the plant-pathogen fungus *Sclerotinia sclerotiorum*. J Gen Virol **87:**241–249. http://dx.doi.org/10.1099/vir.0.81522-0.
14. **Zhang LY, Fu YP, Xie JT, Jiang DH, Li GQ, Yi XH.** 2009. A novel virus that infecting hypovirulent strain XG36-1 of plant fungal pathogen *Sclerotinia sclerotiorum*. Virol J **6:**96. http://dx.doi.org/10.1186/1743-422X-6-96.
15. **Hu ZJ, Wu SS, Cheng JS, Fu YP, Jiang DH, Xie JT.** 2014. Molecular characterization of two positive-strand RNA viruses co-infecting a hypovirulent strain of *Sclerotinia sclerotiorum*. Virology **464:**450–459. http://dx.doi.org/10.1016/j.virol.2014.07.007.
16. **Khalifa ME, Pearson MN.** 2014. Characterisation of a novel hypovirus from *Sclerotinia sclerotiorum* potentially representing a new genus within the *Hypoviridae*. Virology **464-465:**441–449. http://dx.doi.org/10.1016/j.virol.2014.07.005.
17. **Xie JT, Xiao XQ, Fu YP, Liu HQ, Cheng JS, Ghabrial SA, Li GQ, Jiang DH.** 2011. A novel mycovirus closely related to hypoviruses that infects the plant pathogenic fungus *Sclerotinia sclerotiorum*. Virology **418:**49–56. http://dx.doi.org/10.1016/j.virol.2011.07.008.
18. **Jiang D, Fu Y, Guoqing L, Ghabrial SA.** 2013. Viruses of the plant pathogenic fungus *Sclerotinia sclerotiorum*. Adv Virus Res **86:**215–248. http://dx.doi.org/10.1016/B978-0-12-394315-6.00008-8.
19. **Nuss DL.** 2011. Mycoviruses, RNA silencing, and viral RNA recombination. Adv Virus Res **80:**25–48. http://dx.doi.org/10.1016/B978-0-12-385987-7.00002-6.
20. **Wang SC, Kondo H, Liu L, Guo LH, Qiu DW.** 2013. A novel virus in the family *Hypoviridae* from the plant pathogenic fungus Fusarium graminearum. Virus Res **174:**69–77. http://dx.doi.org/10.1016/j.virusres.2013.03.002.
21. **Koloniuk I, El-Habbak MH, Petrzik K, Ghabrial SA.** 2014. Complete genome sequence of a novel hypovirus infecting *Phomopsis longicolla*. Arch Virol **159:**1861–1863. http://dx.doi.org/10.1007/s00705-014-1992-8.
22. **Yaegashi H, Kanematsu S, Ito T.** 2012. Molecular characterization of a new hypovirus infecting a phytopathogenic fungus, *Valsa ceratosperma*. Virus Res **165:**143–150. http://dx.doi.org/10.1016/j.virusres.2012.02.008.
23. **Ghabrial SA, Suzuki N.** 2009. Viruses of plant pathogenic fungi. Annu Rev Phytopathol **47:**353–384. http://dx.doi.org/10.1146/annurev-phyto-080508-081932.
24. **Enebak SA, Macdonald WL, Hillman BI.** 1994. Effect of dsRNA associated with isolates of *Cryphonectria parasitica* from the Central Appalachians and their relatedness to other dsRNAs from North America and Europe. Phytopathology **84:**528–534. http://dx.doi.org/10.1094/Phyto-84-528.
25. **Chen BS, Choi GH, Nuss DL.** 1994. Attenuation of fungal virulence by synthetic infectious hypovirus transcripts. Science **264:**1762–1764. http://dx.doi.org/10.1126/science.8209256.
26. **Chen BS, Nuss DL.** 1999. Infectious cDNA clone of hypovirus CHV1-Euro7: a comparative virology approach to investigate virus-mediated hypovirulence of the chestnut blight fungus *Cryphonectria parasitica*. J Virol **73:**985–992.
27. **Lin HY, Lan XW, Liao H, Parsley TB, Nuss DL, Chen BS.** 2007. Genome sequence, full-length infectious cDNA clone, and mapping of viral double-stranded RNA accumulation determinant of hypovirus CHV1-EP721. J Virol **81:**1813–1820. http://dx.doi.org/10.1128/JVI.01625-06.
28. **Kull LS, Pedersen WL, Palmquist D, Hartman GL.** 2004. Mycelial compatibility grouping and aggressiveness of *Sclerotinia sclerotiorum*. Plant Dis **88:**325–332. http://dx.doi.org/10.1094/PDIS.2004.88.4.325.
29. **Grabherr MG, Haas BJ, Yassour M, Levin JZ, Thompson DA, Amit I, Adiconis X, Fan L, Raychowdhury R, Zeng Q, Chen Z, Mauceli E, Hacohen N, Gnirke A, Rhind N, di Palma F, Birren BW, Nusbaum C, Lindblad-Toh K, Friedman N, Regev A.** 2011. Full-length transcriptome assembly from RNA-Seq data without a reference genome. Nat Biotechnol **29:**644–652. http://dx.doi.org/10.1038/nbt.1883.
30. **Altschul SF, Gish W, Miller W, Myers EW, Lipman DJ.** 1990. Basic local alignment search tool. J Mol Biol **215:**403–410. http://dx.doi.org/10.1016/S0022-2836(05)80360-2.
31. **Edgar RC.** 2004. MUSCLE: multiple sequence alignment with high accuracy and high throughput. Nucleic Acids Res **32:**1792–1797. http://dx.doi.org/10.1093/nar/gkh340.
32. **Tamura K, Dudley J, Nei M, Kumar S.** 2007. MEGA4: Molecular Evolutionary Genetics Analysis (MEGA) software version 4.0. Mol Biol Evol **24:**1596–1599. http://dx.doi.org/10.1093/molbev/msm092.
33. **Nicholas KB, Nicholas HB, Jr, Deerfield DW, II.** 1997. GeneDoc: analysis and visualization of genetic variation. EMBNEW News **4:**14.
34. **Martin DP, Lemey P, Lott M, Moulton V, Posada D, Lefeuvre P.** 2010. RDP3: a flexible and fast computer program for analyzing recombination. Bioinformatics **26:**2462–2463. http://dx.doi.org/10.1093/bioinformatics/btq467.
35. **Etherington GJ, Dicks J, Roberts IN.** 2005. Recombination Analysis Tool (RAT): a program for the high-throughput detection of recombination. Bioinformatics **21:**278–281. http://dx.doi.org/10.1093/bioinformatics/bth500.
36. **Katoh K, Standley DM.** 2013. MAFFT multiple sequence alignment software version 7: improvements in performance and usability. Mol Biol Evol **30:**772–780. http://dx.doi.org/10.1093/molbev/mst010.
37. **Finn RD, Clements J, Eddy SR.** 2011. HMMER web server: interactive sequence similarity searching. Nucleic Acids Res **39:**W29–W37. http://dx.doi.org/10.1093/nar/gkr367.
38. **Fink GR, Styles CA.** 1972. Curing of a killer factor in *Saccharomyces cerevisiae*. Proc Natl Acad Sci U S A **69:**2846–2849. http://dx.doi.org/10.1073/pnas.69.10.2846.
39. **Kohn LM, Stasovski E, Carbone I, Royer J, Anderson JB.** 1991. Mycelial incompatibility and molecular markers identify genetic-variability in field populations of *Sclerotinia sclerotiorum*. Phytopathology **81:**480–485. http://dx.doi.org/10.1094/Phyto-81-480.
40. **Depaulo JJ, Powell CA.** 1995. Extraction of double-stranded RNA from

plant tissues without the use of organic solvents. Plant Dis **79:**246–248. http://dx.doi.org/10.1094/PD-79-0246.
41. **Allemann C, Hoegger P, Heiniger U, Rigling D.** 1999. Genetic variation of Cryphonectria hypoviruses (CHV1) in Europe, assessed using restriction fragment length polymorphism (RFLP) markers. Mol Ecol **8:**843–854. http://dx.doi.org/10.1046/j.1365-294X.1999.00639.x.
42. **Miller LA.** 2001. Microwave processing techniques for biological samples in a service laboratory, p 89–100. *In* Giberson RT, Demaree RS (ed), Microwave techniques and protocols. Humana Press, Totowa, NJ. http://dx.doi.org/10.1007/978-1-59259-128-2_8.
43. **Wilkinson KA, Merino EJ, Weeks KM.** 2006. Selective 2′-hydroxyl acylation analyzed by primer extension (SHAPE): quantitative RNA structure analysis at single nucleotide resolution. Nat Protoc **1:**1610–1616. http://dx.doi.org/10.1038/nprot.2006.249.
44. **Rice GM, Busan S, Karabiber F, Favorov OV, Weeks KM.** 2014. SHAPE analysis of small RNAs and riboswitches. Methods Enzymol **549:**165–187. http://dx.doi.org/10.1016/B978-0-12-801122-5.00008-8.
45. **Karabiber F, McGinnis JL, Favorov OV, Weeks KM.** 2013. QuShape: rapid, accurate, and best-practices quantification of nucleic acid probing information, resolved by capillary electrophoresis. RNA **19:**63–73. http://dx.doi.org/10.1261/rna.036327.112.
46. **Zuker M.** 2003. Mfold web server for nucleic acid folding and hybridization prediction. Nucleic Acids Res **31:**3406–3415. http://dx.doi.org/10.1093/nar/gkg595.
47. **Khalifa ME, Pearson MN.** 2014. Molecular characterisation of an endornavirus infecting the phytopathogen *Sclerotinia sclerotiorum*. Virus Res **189:**303–309. http://dx.doi.org/10.1016/j.virusres.2014.06.010.
48. **Dodds JA.** 1980. Association of type-1 viral-like dsRNA with club-shaped particles in hypovirulent strains of *Endothia parasitica*. Virology **107:**1–12. http://dx.doi.org/10.1016/0042-6822(80)90267-6.
49. **Newhouse JR, Hoch HC, Macdonald WL.** 1983. The ultrastructure of *Endothia parasitica*. Comparison of a virulent with a hypovirulent isolate. Can J Bot **61:**389–399. http://dx.doi.org/10.1139/b83-046.
50. **Newhouse JR, Macdonald WL, Hoch HC.** 1990. Virus-like particles in hyphae and conidia of European hypovirulent (dsRNA-containing) strains of *Cryphonectria parasitica*. Can J Bot **68:**90–101. http://dx.doi.org/10.1139/b90-013.
51. **Adams IP, Glover RH, Monger WA, Mumford R, Jackeviciene E, Navalinskiene M, Samuitiene M, Boonham N.** 2009. Next-generation sequencing and metagenomic analysis: a universal diagnostic tool in plant virology. Mol Plant Pathol **10:**537–545. http://dx.doi.org/10.1111/j.1364-3703.2009.00545.x.
52. **Coetzee B, Freeborough M-J, Maree HJ, Celton J-M, Rees DJG, Burger JT.** 2010. Deep sequencing analysis of viruses infecting grapevines: virome of a vineyard. Virology **400:**157–163. http://dx.doi.org/10.1016/j.virol.2010.01.023.
53. **Kristensen DM, Mushegian AR, Dolja VV, Koonin EV.** 2010. New dimensions of the virus world discovered through metagenomics. Trends Microbiol **18:**11–19. http://dx.doi.org/10.1016/j.tim.2009.11.003.
54. **Rosario K, Breitbart M.** 2011. Exploring the viral world through metagenomics. Curr Opin Virol **1:**289–297. http://dx.doi.org/10.1016/j.coviro.2011.06.004.
55. **Marvelli RA, Hobbs HA, Li S, McCoppin NK, Domier LL, Hartman GL, Eastburn DM.** 6 September 2013. Identification of novel double-stranded RNA mycoviruses of *Fusarium virguliforme* and evidence of their effects on virulence. Arch Virol http://dx.doi.org/10.1007/s00705-013-1760-1.
56. **Al Rwahnih M, Daubert S, Urbez-Torres JR, Cordero F, Rowhani A.** 2011. Deep sequencing evidence from single grapevine plants reveals a virome dominated by mycoviruses. Arch Virol **156:**397–403. http://dx.doi.org/10.1007/s00705-010-0869-8.
57. **Shapira R, Choi GH, Hillman BI, Nuss DL.** 1991. The contribution of defective RNAs to the complexity of viral-encoded double-stranded RNA populations present in hypovirulent strains of the chestnut blight fungus *Cryphonectria parasitica*. EMBO J **10:**741–746.
58. **Nuss DL, Hillman BI.** 2012. Family *Hypoviridae*, p 1029–1033. *In* King AMQ, Adams MJ, Carstens EB, Lefkowitz EJ (ed), Virus taxonomy: classification and nomenclature of viruses; ninth report of the International Committee on Taxonomy of Viruses. Elsevier Academic Press, Waltham, MA.
59. **Fahima T, Kazmierczak P, Hansen DR, Pfeiffer P, Vanalfen NK.** 1993. Membrane-associated replication of an unencapsidated double-strand RNA of the fungus, *Cryphonectria parasitica*. Virology **195:**81–89. http://dx.doi.org/10.1006/viro.1993.1348.
60. **Suzuki N, Nuss DL.** 2002. Contribution of protein p40 to hypovirus-mediated modulation of fungal host phenotype and viral RNA accumulation. J Virol **76:**7747–7759. http://dx.doi.org/10.1128/jvi.76.15.7747-7759.2002.
61. **Lefebvre A, Scalla R, Pfeiffer P.** 1990. The double-stranded RNA associated with the 447 cytoplasmic male-sterility in *Vicia faba* is packaged together with its replicase in cytoplasmic membranous vesicles. Plant Mol Biol **14:**477–490. http://dx.doi.org/10.1007/bf00027494.
62. **Moriyama H, Kanaya K, Wang JZ, Nitta T, Fukuhara T.** 1996. Stringently and developmentally regulated levels of a cytoplasmic double-stranded RNA and its high-efficiency transmission via egg and pollen in rice. Plant Mol Biol **31:**713–719. http://dx.doi.org/10.1007/bf00019459.
63. **Pearson MN, Beever RE, Boine B, Arthur K.** 2009. Mycoviruses of filamentous fungi and their relevance to plant pathology. Mol Plant Pathol **10:**115–128. http://dx.doi.org/10.1111/j.1364-3703.2008.00503.x.
64. **Gibbs A, Ohshima K.** 2010. Potyviruses and the digital revolution. Annu Rev Phytopathol **48:**205–223. http://dx.doi.org/10.1146/annurev-phyto-073009-114404.
65. **Tomimura K, Spak J, Katis N, Jenner CE, Walsh JA, Gibbs AJ, Ohshima K.** 2004. Comparisons of the genetic structure of populations of *Turnip mosaic virus* in West and East Eurasia. Virology **330:**408–423. http://dx.doi.org/10.1016/j.virol.2004.09.040.
66. **Ohshima K, Tomitaka Y, Wood JT, Minematsu Y, Kajiyama H, Tomimura K, Gibbs AJ.** 2007. Patterns of recombination in turnip mosaic virus genomic sequences indicate hotspots of recombination. J Gen Virol **88:**298–315. http://dx.doi.org/10.1099/vir.0.82335-0.
67. **Pinel-Galzi A, Mpunami A, Sangu E, Rakotomalala M, Traore O, Sereme D, Sorho F, Sere Y, Kanyeka Z, Konate G, Fargette D.** 2009. Recombination, selection and clock-like evolution of *Rice yellow mottle virus*. Virology **394:**164–172. http://dx.doi.org/10.1016/j.virol.2009.08.008.
68. **Mu R, Romero TA, Hanley KA, Dawe AL.** 2011. Conserved and variable structural elements in the 5′ untranslated region of two hypoviruses from the filamentous fungus *Cryphonectria parasitica*. Virus Res **161:**203–208. http://dx.doi.org/10.1016/j.virusres.2011.07.023.
69. **Nagy PD, Simon AE.** 1997. New insights into the mechanisms of RNA recombination. Virology **235:**1–9. http://dx.doi.org/10.1006/viro.1997.8681.
70. **Draghici HK, Varrelmann M.** 2010. Evidence for similarity-assisted recombination and predicted stem-loop structure determinant in potato virus X RNA recombination. J Gen Virol **91:**552–562. http://dx.doi.org/10.1099/vir.0.014712-0.
71. **Chen YK, Goldbach R, Prins M.** 2002. Inter- and intramolecular recombinations in the *Cucumber mosaic virus* genome related to adaptation to alstroemeria. J Virol **76:**4119–4124. http://dx.doi.org/10.1128/jvi.76.8.4119-4124.2002.
72. **Sun Q, Choi GH, Nuss DL.** 2009. A single Argonaute gene is required for induction of RNA silencing antiviral defense and promotes viral RNA recombination. Proc Natl Acad Sci U S A **106:**17927–17932. http://dx.doi.org/10.1073/pnas.0907552106.
73. **Sun L, Suzuki N.** 2008. Intragenic rearrangements of a mycoreovirus induced by the multifunctional protein p29 encoded by the prototypic hypovirus CHV1-EP713. RNA **14:**2557–2571. http://dx.doi.org/10.1261/rna.1125408.
74. **Chen BS, Geletka LM, Nuss DL.** 2000. Using chimeric hypoviruses to fine-tune the interaction between a pathogenic fungus and its plant host. J Virol **74:**7562–7567. http://dx.doi.org/10.1128/jvi.74.16.7562-7567.2000.
75. **Craven MG, Pawlyk DM, Choi GH, Nuss DL.** 1993. Papain-like protease p29 as a symptom determinant encoded by a hypovirulence-associated virus of the chestnut blight fungus. J Virol **67:**6513–6521.
76. **Segers GC, Zhang X, Deng F, Sun Q, Nuss DL.** 2007. Evidence that RNA silencing functions as an antiviral defense mechanism in fungi. Proc Natl Acad Sci U S A **104:**12902–12906. http://dx.doi.org/10.1073/pnas.0702500104.
77. **Anandalakshmi R, Pruss GJ, Ge X, Marathe R, Mallory AC, Smith TH, Vance VB.** 1998. A viral suppressor of gene silencing in plants. Proc Natl Acad Sci U S A **95:**13079–13084. http://dx.doi.org/10.1073/pnas.95.22.13079.
78. **Suzuki N, Chen BS, Nuss DL.** 1999. Mapping of a hypovirus p29 protease symptom determinant domain with sequence similarity to potyvirus HC-Pro protease. J Virol **73:**9478–9484.
79. **Shimizu T, Ito T, Kanematsu S.** 2014. Functional analysis of a melanin biosynthetic gene using RNAi-mediated gene silencing in *Rosellinia neca-*

trix. Fungal Biol **118:**413–421. http://dx.doi.org/10.1016/j.funbio.2014.02.006.
80. **Willetts HJ, Bullock S.** 1992. Developmental biology of sclerotia. Mycol Res **96:**801–816. http://dx.doi.org/10.1139/b68-124.
81. **Kanematsu S, Shimizu T, Salaipeth L, Yaegashi H, Sasaki A, Ito T, Suzuki N.** 2014. Genome rearrangement of a mycovirus Rosellinia necatrix megabirnavirus 1 affecting its ability to attenuate virulence of the host fungus. Virology **450:**308–315. http://dx.doi.org/10.1016/j.virol.2013.12.002.
82. **Paoletti M, Saupe SJ.** 2009. Fungal incompatibility: evolutionary origin in pathogen defense? Bioessays **31:**1201–1210. http://dx.doi.org/10.1002/bies.200900085.
83. **Kohli Y, Morrall RAA, Anderson JB, Kohn LM.** 1992. Local and trans-Canadian clonal distribution of *Sclerotinia sclerotiorum* on canola. Phytopathology **82:**875–880. http://dx.doi.org/10.1094/Phyto-82-875.
84. **Brusini J, Robin C.** 2013. Mycovirus transmission revisited by *in situ* pairings of vegetatively incompatible isolates of *Cryphonectria parasitica*. J Virol Methods **187:**435–442. http://dx.doi.org/10.1016/j.jviromet.2012.11.025.
85. **Choi GH, Dawe AL, Churbanov A, Smith ML, Milgroom MG, Nuss DL.** 2012. Molecular characterization of vegetative incompatibility genes that restrict hypovirus transmission in the chestnut blight fungus *Cryphonectria parasitica*. Genetics **190:**113–127. http://dx.doi.org/10.1534/genetics.111.133983.
86. **Zhang DX, Spiering MJ, Dawe AL, Nuss DL.** 2014. Vegetative incompatibility loci with dedicated roles in allorecognition restrict mycovirus transmission in chestnut blight fungus. Genetics **197:**701–714. http://dx.doi.org/10.1534/genetics.114.164574.
87. **Amselem J, Cuomo CA, van Kan JAL, Viaud M, Benito EP, Couloux A, Coutinho PM, de Vries RP, Dyer PS, Fillinger S, Fournier E, Gout L, Hahn M, Kohn L, Lapalu N, Plummer KM, Pradier J-M, Quévillon E, Sharon A, Simon A, ten Have A, Tudzynski B, Tudzynski P, Wincker P, Andrew M, Anthouard V, Beever RE, Beffa R, Benoit I, Bouzid O, Brault B, Chen Z, Choquer M, Collémare J, Cotton P, Danchin EG, Da Silva C, Gautier A, Giraud C, Giraud T, Gonzalez C, Grossetete S, Güldener U, Henrissat B, Howlett BJ, Kodira C, Kretschmer M, Lappartient A, Leroch M, Levis C, Mauceli E, Neuvéglise C, Oeser B, Pearson M, Poulain J, Poussereau N, Quesneville H, Rascle C, Schumacher J, Ségurens B, Sexton A, Silva E, Sirven C, Soanes DM, Talbot NJ, Templeton M, Yandava C, Yarden O, Zeng Q, Rollins JA, Lebrun M-H, Dickman M.** 2011. Genomic analysis of the necrotrophic fungal pathogens *Sclerotinia sclerotiorum* and *Botrytis cinerea*. PLoS Genet **7:**e1002230. http://dx.doi.org/10.1371/journal.pgen.1002230.
88. **Attanayake RN, Carter PA, Jiang DH, del Rio-Mendoza L, Chen WD.** 2013. *Sclerotinia sclerotiorum* populations infecting canola from China and the United States are genetically and phenotypically distinct. Phytopathology **103:**750–761. http://dx.doi.org/10.1094/phyto-07-12-0159-r.
89. **Ekins MG, Hayden HL, Aitken EAB, Goulter KC.** 2011. Population structure of *Sclerotinia sclerotiorum* on sunflower in Australia. Australas Plant Pathol **40:**99–108. http://dx.doi.org/10.1007/s13313-010-0018-6.
90. **Litholdo Júnior CG, Gomes EV, Lobo Júnior M, Nasser LCB, Petrofeza S.** 2011. Genetic diversity and mycelial compatibility groups of the plant-pathogenic fungus *Sclerotinia sclerotiorum* in Brazil. Genet Mol Res **10:**868–877. http://dx.doi.org/10.4238/vol10-2gmr937.
91. **Mert-Turk F, Ipek M, Mermer D, Nicholson P.** 2007. Microsatellite and morphological markers reveal genetic variation within a population of *Sclerotinia sclerotiorum* from oilseed rape in the Canakkale Province of Turkey. J Phytopathol **155:**182–187. http://dx.doi.org/10.1111/j.1439-0434.2007.01223.x.